

# Removal of Dilute Nitrogen Oxide by the Absorption in Mn–Zr Oxide

Koichi Eguchi,\* Mitsunori Watabe, Shigeki Ogata, and Hiromichi Arai

Department of Materials Science and Technology, Graduate School of Engineering Sciences,  
Kyushu University 39, 6-1, Kasuga-Koen, Kasuga, Fukuoka 816

(Received October 27, 1994)

The removal of NO by absorption in manganese zirconium oxide (Mn–Zr oxide) was investigated in both the presence and absence of gaseous O<sub>2</sub>. The Mn–Zr oxide at Mn/Zr=1 exhibited a high NO absorption rate and capacity at 200 °C. The absorption was promoted in the presence of O<sub>2</sub>. The absorption capacity was not strongly affected by the NO concentration (75–900 ppm) and *W/F* (0.125–1 g s cm<sup>-3</sup>). An infrared analysis of the absorbed species indicated that the absorption proceeds as the formation of nitrate in the bulk solid. The absorption and desorption were reversible, and the oxide solid was recovered upon heating a preabsorbed sample at 400 °C. Although the amorphous phase of the Mn–Zr oxide which is formed after heating at 450 °C is effective for NO absorption, due to good mixing of manganese oxide and zirconium oxide, heating at higher temperatures (≥550 °C), leading to a decrease in the surface area and crystallization of single oxides, resulted in a decrease in the absorption capacity. NO removal appears to proceed by the oxidation of NO on the Mn sites, and a subsequent absorption at the Zr sites as (NO<sub>3</sub>)<sup>-</sup> species.

The removal of NO<sub>x</sub> from exhaust gases is important for solving acid-rain and air-pollution problems. The selective reduction of NO<sub>x</sub> with hydrocarbons has recently been actively investigated for diesel and lean-fuel engines as well as cogeneration systems.<sup>1,2)</sup> This catalytic process, however, has not yet been commercialized, mainly due to catalyst deactivation by the coexisting gases, such as H<sub>2</sub>O and SO<sub>2</sub>.<sup>3,4)</sup> This difficulty is partly related to the very dilute concentration of NO<sub>x</sub> in exhaust gases. We have proposed to overcome this difficulty by combining the separation process of NO<sub>x</sub> from the coexisting gas with catalytic NO<sub>x</sub> conversion. Since the conversion catalysts for concentrated NO<sub>x</sub> have already been well-developed, the selective separation of dilute NO<sub>x</sub> from a gaseous mixture must be improved. The present investigation aims to remove dilute NO<sub>x</sub> from gaseous mixtures, and producing concentrated nitrogen oxides by absorption–desorption cycles of the solid. The reversible absorption of NO<sub>x</sub> in solids has so far been reported for the Y–Ba–Cu–O,<sup>5)</sup> Ba–Cu–O,<sup>6)</sup> and Y–Sr–Co–O<sup>7)</sup> systems. Although these oxides have been reported to be active for removing of a large amount of NO<sub>x</sub> by absorption, a deactivation of absorbents is expected because of the formation of surface carbonate in the presence of CO<sub>2</sub> on rare-earth or alkaline-earth components. We have recently reported on the development of manganese zirconium oxide (Mn–Zr oxide) materials for NO<sub>x</sub> absorption, which was not affected by the presence of CO<sub>2</sub>.<sup>8)</sup> In this paper, the absorption–desorption properties and mechanism of the Mn–Zr oxides for NO removal are

considered in terms of exhaust cleaning.

## Experimental

**Sample Preparation.** Mixed-oxide samples were generally prepared by coprecipitation from a solution of the corresponding nitrate mixture. For preparing Mn–Zr oxides, the calculated amount of Mn(NO<sub>3</sub>)<sub>3</sub>·6H<sub>2</sub>O and ZrO(NO<sub>3</sub>)<sub>2</sub>·2H<sub>2</sub>O (Kishida Chemical, Guaranteed reagent grade) was dissolved in water. After adding ammonia water to the nitrate solution, a solution with the precipitate was first evaporated to dryness, and then heated at 450 °C for 6 h in air. The thus-obtained powder was sieved to 10–20 mesh.

In comparison with the standard preparation procedure of coprecipitation from nitrate, the Mn–Zr oxide was prepared by three different routes. Coprecipitation from an acetate solution was carried out by adding ammonia water to an aqueous solution (400 ml) of Mn(CH<sub>3</sub>COO)<sub>3</sub> (6.53 g) and Zr(CH<sub>3</sub>COO)<sub>4</sub> (6.00 g). The precipitate was also heated at 450 °C for 6 h in air. The precursor method was employed for preparing Mn–Zr oxide. Citric acid was added to a 0.087 mol dm<sup>-3</sup> solution containing Mn(NO<sub>3</sub>)<sub>3</sub> and ZrO(NO<sub>3</sub>)<sub>2</sub>. The thus-obtained precursor gel was heated using the same procedure as that in the coprecipitation process. The Mn–Zr oxide was prepared from the hydrolysis of metal alkoxides. Manganese diisopropoxide (1.05 g) and zirconium tetraisopropoxide (2.00 g) (TRI Chemical Laboratory) were first dissolved in isopropanol (200 ml); water (2 ml) was then added to the alcoholic solution. The resultant gel was dried and calcined at 450 °C for 6 h.

The Mn–Zr oxide was supported on an alumina support by an impregnation process.  $\gamma$ -alumina powder (5.91 g) (Catalysis Soc. Jpn., ALO-4) was suspended in a 2.52×10<sup>-3</sup>

mol dm<sup>-3</sup> aqueous solution of Mn(NO<sub>3</sub>)<sub>3</sub>·6H<sub>2</sub>O and ZrO-(NO<sub>3</sub>)<sub>2</sub>·2H<sub>2</sub>O. After the suspension had been evaporated to dryness, the powder was treated by the same procedure as that of unsupported samples. The loading of the Mn-Zr oxide was 3.5 wt%.

#### NO Removal Experiment and Characterization.

Absorption and desorption experiments of NO were carried out in a flow system. Nitrogen monoxide was diluted in He and mixed with O<sub>2</sub> before being supplied to a quartz tube reactor. The absorption and desorption characteristics of NO<sub>x</sub> were tested over a temperature range from 200 to 400 °C at a contact time of 0.125–1.0 g s cm<sup>-3</sup>. The NO<sub>x</sub> concentration was analyzed using a chemical luminescence-type NO<sub>x</sub> meter (Shimadzu, NOA305). The effluent gas was generally passed through a carbon catalyst in order to reduce NO<sub>2</sub> when analyzing a NO+NO<sub>2</sub> concentration. Only when the NO concentration was necessary the sample gas was directly introduced to the NO<sub>x</sub> meter. The gaseous composition of the inlet and outlet mixture was also analyzed by gas chromatography.

The absorption state of NO<sub>x</sub> was monitored using an FT-IR spectrometer (Shimadzu, FT-IR 8200D). The phase in the sample was identified using an X-ray diffractometer (Rigaku, RINT-1400).

### Results and Discussion

**Absorption of NO by Mn-Zr Oxide.** We previously reported that some oxides are effective in removing dilute NO<sub>x</sub> in air by absorption in a solid.<sup>6,8)</sup> The Mn-Zr oxide system exhibited a high removal of dilute NO in air. Nitrogen monoxide removal of Mn-Zr oxide with different compositions was tested, as shown in Fig. 1. A gaseous mixture containing 900 ppm NO and 10% O<sub>2</sub> was supplied to the oxide sample at 200 °C. Although the outlet concentration of NO was almost zero in every case at the beginning of supplying the gaseous mixture, no nitrogen-containing species were detected during this period based on an outlet-gas analysis by gas

chromatography. The removal of NO sharply decreased with time after 10–30 min from starting the reaction, then gradually approached zero. The total amount of absorbed NO, estimated from integrating the removal curve, was largest for a sample with Mn/Zr=1. The amount of NO removal (0.08 mol/mol-Zr for Mn/Zr=1) was so large that the NO uptake was not merely due to adsorption on the surface, but the absorption of NO in the bulk was operative. The absence of any nitrogen-containing species in the outlet gas also indicates that the removal proceeded by the absorption of NO in the bulk of the oxide sample, and eliminated any possibility of the catalytic decomposition of NO. The absorbed NO was found to be released upon heating of a preabsorbed sample at 400 °C.

A gravimetric analysis during NO removal by the Mn-Zr oxide (Mn/Zr=1) was carried out in 900 ppm NO+10% O<sub>2</sub> at 200 °C. The NO removal accompanied a significant weight increase of the Mn-Zr oxide. The cumulative increase for the initial 90 min of NO removal amounted to 0.047 mol-NO<sub>3</sub>/mol-Zr (1.43 wt% of the initial weight), which was on the same order as the NO removal obtained from the gas-phase analysis. Since the number of Zr atoms exposed at the surface could be roughly estimated from the surface area (ca. 180 m<sup>2</sup> g<sup>-1</sup>) and the general packing densities for cleaved surfaces of oxide crystals to be 10<sup>-5</sup>–10<sup>-4</sup> of that in the bulk, the NO uptake observed in the present system was too large to consider as surface adsorption, and appears to correspond to the absorption in the bulk of the oxide.

The reversibility of the absorption and desorption of the Mn-Zr oxide was tested by repeating the absorption of NO at 200 °C and desorption at 400 °C in He, as shown in Fig. 2. The absorption behavior was basically the same as shown in Fig. 1, except for the difference in

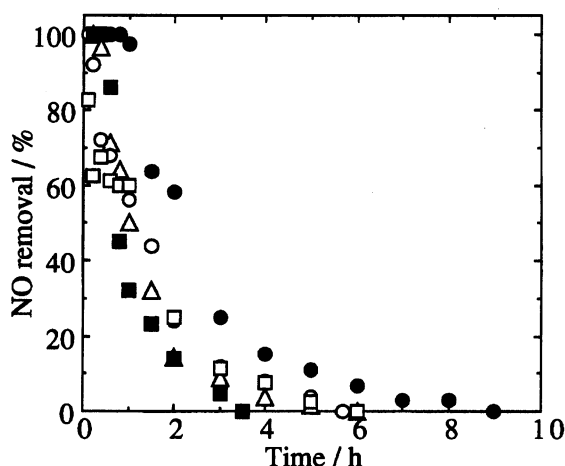


Fig. 1. NO removal of Mn-Zr oxide with different Mn/Zr ratios.  $T=200\text{ }^{\circ}\text{C}$ , 900 ppm NO, 10% O<sub>2</sub>, He balance,  $W/F=1\text{ g s cm}^{-3}$ .  $\triangle$  Mn/Zr=1/9,  $\circ$  Mn/Zr=1/5,  $\bullet$  Mn/Zr=1,  $\square$  Mn/Zr=5,  $\blacksquare$  Mn/Zr=9.

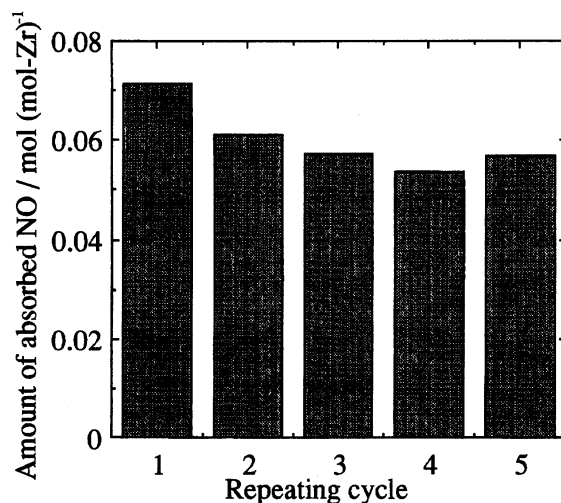
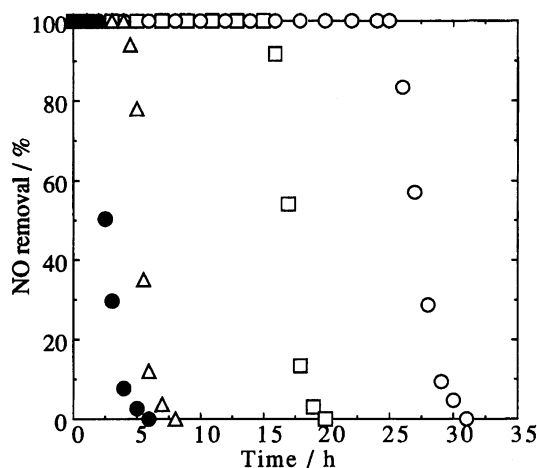


Fig. 2. Amount of absorbed NO after heating of Mn-Zr oxide at 400 °C.  $T=200\text{ }^{\circ}\text{C}$ , 900 ppm NO, 10% O<sub>2</sub>, He balance,  $W/F=1\text{ g s cm}^{-3}$ .

the overall amount of absorption. Although the absorption capacity of the first absorption experiment after a heat treatment at 450 °C was the largest, it then decreased and was almost stabilized from the 2nd cycle, indicating that the absorption and thermal desorption was almost reversible. The absorption amount at the fifth absorption step decreased to ca. 85% of that at the first step. This decrease may have resulted from a decrease in the surface area, or grain growth of manganese oxide and zirconium oxide.

**Effect of Gaseous Composition and Contact Time on the Removal of NO.** The removal of NO from the O<sub>2</sub>-containing gas was tested at different concentrations of NO (Fig. 3). The initial removal of NO was 100% at every NO concentration. When dilute NO of 75 ppm was supplied to the Mn-Zr oxide, the NO removal was maintained at a high level for a long period. Although the overall absorption capacity decreased only slightly with decreasing NO concentration, it was not strongly affected by the concentration of NO under the present experimental condition.

The effect of the O<sub>2</sub> concentration in the gas phase on the overall absorption capacity was tested (Fig. 4). The initial removal of NO was 100% for every concentration of O<sub>2</sub> at 0–10%. The absorption capacity attained during 6 h of absorption operation remained almost unchanged when the atmosphere contained O<sub>2</sub>. However, for the absorption experiment with NO in commercial He, the absorption capacity was significantly smaller than in the case of O<sub>2</sub>-containing atmospheres. This means that the presence of gaseous oxygen is important in the absorption of NO. Based on the previous result for the Ba-Cu oxide system,<sup>6)</sup> NO molecules are ex-



symbol	○	□	△	●
NO conc. / ppm	75	150	450	900
mol-NO uptake / mol-Zr	0.068	0.083	0.082	0.082

Fig. 3. Effect of NO concentration on NO removal of Mn-Zr oxide.  $T=200\text{ }^{\circ}\text{C}$ , 10% O<sub>2</sub>, He balance,  $W/F=1\text{ g s cm}^{-3}$ , NO concentration: ○ 75 ppm, □ 150 ppm, △ 450 ppm, ● 900 ppm.

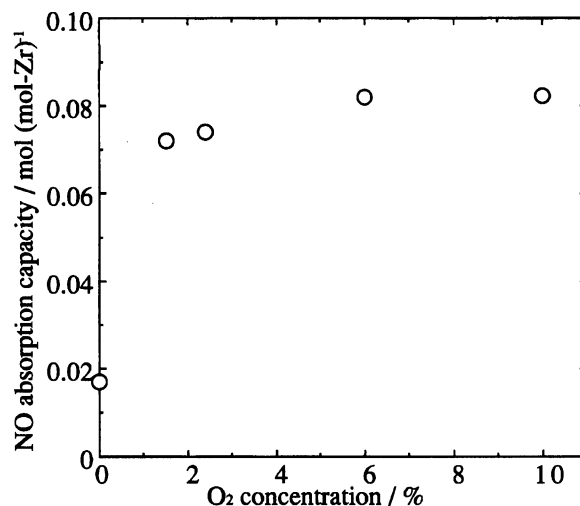
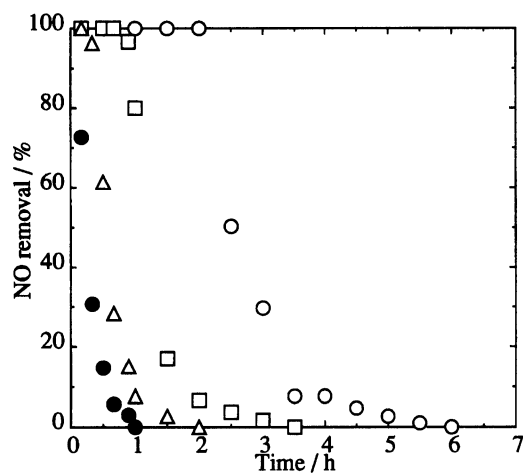


Fig. 4. Effect of oxygen concentration on NO absorption capacity of Mn-Zr oxide.  $T=200\text{ }^{\circ}\text{C}$ , 900 ppm NO, 10% O<sub>2</sub>, He balance,  $W/F=1\text{ g s cm}^{-3}$ .

pected to be oxidized on the surface of Mn-Zr oxide and retained in the solid as nitrate ions. Even when commercially available He was supplied to the Mn-Zr oxide and a relatively small amount of NO (0.017 mol/mol-Zr) was absorbed. In this case, oxygen appears to have been supplied not only from impurity O<sub>2</sub> in commercial He, but also from the lattice of the Mn oxide accompanied by the reduction of Mn ions, since the valence of Mn is very sensitive to the atmosphere. Thus, the absorption proceeded until the available lattice oxygen was consumed for the oxidation of NO.

The effect of the contact time ( $W/F$ ) was also investigated, as shown in Fig. 5, where  $W$  is the weight of the Mn-Zr oxide and  $F$  is the total flow rate. NO removal was 100% for contact times of 1.0, 0.5, and 0.25 g s cm<sup>-3</sup> at the start of absorption, whereas it decreased sharply in the case of  $W/F=0.125\text{ g s cm}^{-3}$ . The amount of absorption per Zr ion, on the other hand, was not strongly affected by  $W/F$ . Since a large flow rate led to a rapid saturation of absorption, the total absorption capacity was unchanged with  $W/F$ . The contact time and NO concentration did not affect the overall absorption capacity under the present experimental conditions, and the initial NO removal was high in every case. Therefore, the absorption was regarded as being very rapid. Such rapid absorption is favorable regarding practical applications of the NO-removal system.

**Effect of the Calcination Temperature for Mn-Zr Oxide.** Mn-Zr oxide was calcined at different temperatures and subjected to the absorption experiment shown in Fig. 6. NO absorption was observable for Mn-Zr oxide (Mn/Zr=1) calcined at different temperatures; however, the amount of absorption was quite different depending on the heat-treatment temperature. The overall amount of absorption was maximum for a sample heated at 450 °C, but decreased along with ei-



symbol	●	△	□	○
W / F / g s cm <sup>-3</sup>	0.125	0.25	0.5	1
mol-NO uptake / mol-Zr	0.076	0.069	0.075	0.082

Fig. 5. Effect of contact time on NO removal of Mn-Zr oxide.  $T=200^{\circ}\text{C}$ , 900 ppm NO, 10%  $\text{O}_2$ , He balance,  $W/F$ : ●  $0.125\text{ g s cm}^{-3}$ , △  $0.25\text{ g s cm}^{-3}$ , □  $0.5\text{ g s cm}^{-3}$ , ○  $1\text{ g s cm}^{-3}$ .

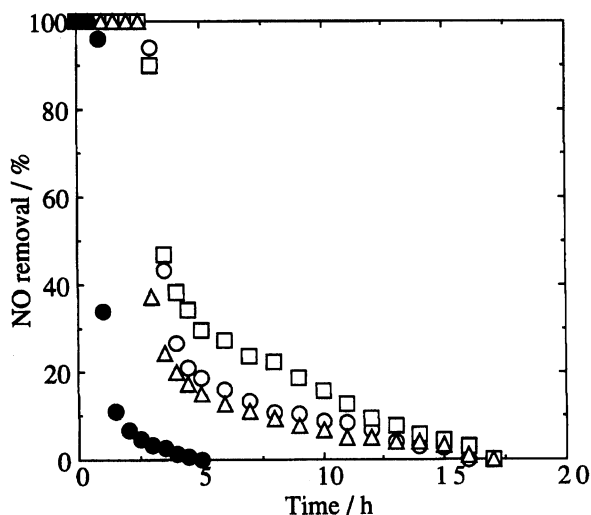


Fig. 6. Effect of calcination temperature on NO removal of Mn-Zr oxide (Mn/Zr=1).  $T=200^{\circ}\text{C}$ , 900 ppm NO, 10%  $\text{O}_2$ , He balance,  $W/F=1\text{ g s cm}^{-3}$ . Heat treatment: ○  $350^{\circ}\text{C}$  for 6 h, □  $450^{\circ}\text{C}$  for 6 h, △  $550^{\circ}\text{C}$  for 6 h, ●  $650^{\circ}\text{C}$  for 6 h.

ther increasing or decreasing the calcination temperature.

The effect of the calcination temperature was investigated based on a phase analysis by X-ray diffraction (Fig. 7). The Mn-Zr oxide sample (Mn/Zr=1) heated at  $350^{\circ}\text{C}$  showed no obvious diffraction lines except for a broad halo around  $2\theta=30^{\circ}$ . As the calcination temperature increased, the diffraction lines grew to form the crystalline  $\text{Mn}_2\text{O}_3$  phase from  $450^{\circ}\text{C}$ , and were sharpened and intensified with increasing temperature. On the contrary, the halo from the amorphous body

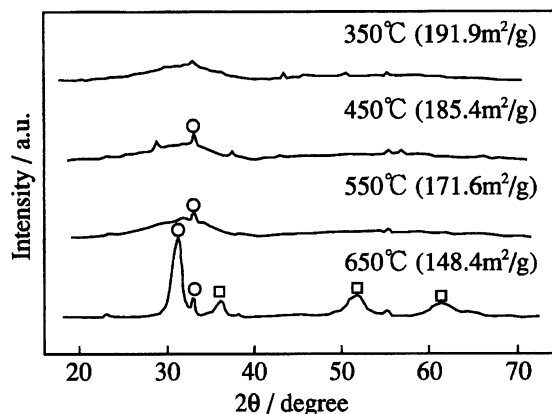


Fig. 7. XRD pattern of Mn-Zr oxide after calcination. Values in parentheses are surface areas of the samples. ○  $\text{Mn}_2\text{O}_3$ , □  $\text{ZrO}_2$ .

was weakened. The sharp diffraction lines after heating at  $650^{\circ}\text{C}$  were attributed to  $\text{Mn}_2\text{O}_3$  and  $\text{ZrO}_2$  phases. The surface areas of the samples are also listed in the figure. The surface area was very high at low calcination temperature ( $>180\text{ m}^2\text{ g}^{-1}$ ), but decreased accompanied by crystal growth and sintering of the oxide.

The X-ray diffraction data indicate that the equilibrium phase at this composition represents a coexisting 2 phases of manganese oxide and zirconium oxide. The valence of Zr appears to be 4+, whereas that of Mn may be very sensitive to both the atmosphere and temperature. Considering the phase and surface area at each calcination temperature, the decrease in the absorption capacity at high calcination temperature is due to the crystallization of the sample and phase separation into two oxides as the system is equilibrated. The good mixing of the Mn and Zr components in the amorphous phase is expected to be important for a high absorption capacity of NO. The decrease in the surface area also appears to retard absorption, since the absorption initiates from the surface oxidation of NO. However, a low-temperature calcination, e.g., at  $350^{\circ}\text{C}$ , was also ineffective for NO absorption due to the following reason.

The thermogravimetric curve of the Mn-Zr oxide (Mn/Zr=1) before calcination indicated that the weight decrease started from  $100^{\circ}\text{C}$ , and came to completion at  $600^{\circ}\text{C}$ . This weight decrease is attributed to the decomposition of nitrate and the elimination of water from the solid, as explained later. Since a relatively large amount of NO is still contained in the solid at  $350^{\circ}\text{C}$  in air, calcination at this temperature is not sufficient to decompose the nitrate. These results indicate that a heat treatment at around  $400$ – $450^{\circ}\text{C}$  is the optimum to attain large NO absorption.

**Mechanism of NO Absorption.** The removal of NO by Mn-Zr oxide can be explained by the absorption of oxidized  $\text{NO}_x$  species in the solid bulk, as already mentioned, judging from the large NO uptake without producing any nitrogen-containing species or weight in-

crease accompanied by removal. Therefore, the infrared spectra were recorded both before and after the absorption of NO (Fig. 8) in order to observe the  $\text{NO}_x$  species in the Mn-Zr oxide. After freshly prepared Mn-Zr oxide was heated at 450 °C, a weak band was observed at 1384  $\text{cm}^{-1}$ . Upon exposure to NO at 200 °C, although no new absorption band appeared, the band at 1384  $\text{cm}^{-1}$  was significantly intensified, and was grown with prolonged absorption. Even after exposure to NO and  $\text{O}_2$  for 90 min at 200 °C, a subsequent heating treatment at 400 °C in He significantly weakened the peak at 1384  $\text{cm}^{-1}$  due to desorption of the  $\text{NO}_x$  species. The band at 1384  $\text{cm}^{-1}$  is characteristic of metal nitrates, and can be attributed to the  $(\text{NO}_3)^-$  species on or in the solid.<sup>9)</sup> Zirconium nitrate oxide,  $\text{ZrO}(\text{NO}_3)_2$ , also exhibited a sharp IR band at 1384  $\text{cm}^{-1}$ . The absorption of NO is expected to be initiated by the oxidation of NO to  $\text{NO}_2$  on the oxide surface, and subsequently proceed by accumulation of  $(\text{NO}_3)^-$  ions in the solid. The absorbed NO is therefore released from the solid by the thermal decomposition of the nitrate ion.

The role of two metallic components in the Mn-Zr oxide was further investigated. The temperature dependence of the catalytic activity of manganese oxide for the oxidation of NO is shown in Fig. 9. The solid line in the figure is the equilibrium conversion of NO at 10%. Since the activity of Mn oxide was high enough to attain equilibrium conversion, the Mn species in the Mn-Zr oxide are expected to serve as catalysts for the oxidation of NO to  $\text{NO}_2$ . Nitrogen dioxide appears to be the intermediate to form  $\text{NO}_3^-$  species.

TG and DTA curves of  $\text{ZrO}(\text{NO}_3)_2 \cdot 2\text{H}_2\text{O}$  are shown in Fig. 10. The weight decrease below 230 °C is very

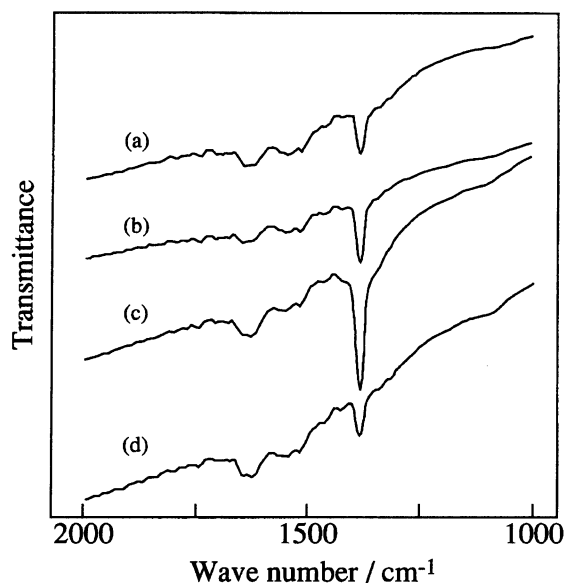


Fig. 8. FT-IR spectra of Mn-Zr oxide. (a) before NO absorption. (b) after NO absorption at 200 °C for 15 min. (c) after NO absorption at 200 °C for 90 min. (d) after heating sample (c) at 400 °C.

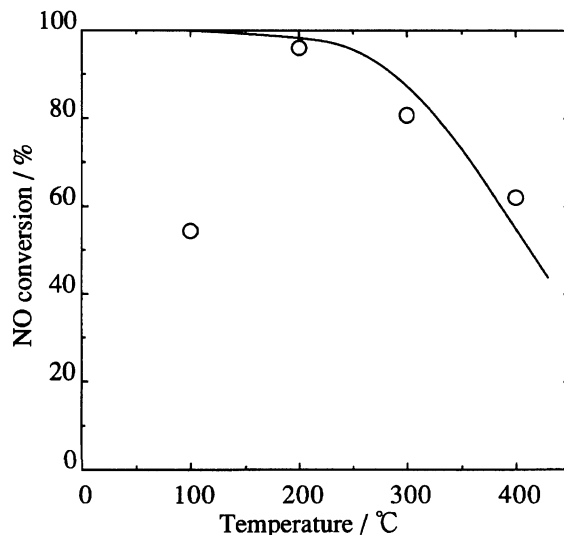


Fig. 9. Temperature dependence of conversion over Mn oxide catalyst for oxidation of NO to  $\text{NO}_2$ . 900 ppm NO, 10%  $\text{O}_2$ , He balance,  $W/F=1 \text{ g s cm}^{-3}$ . — equilibrium conversion.

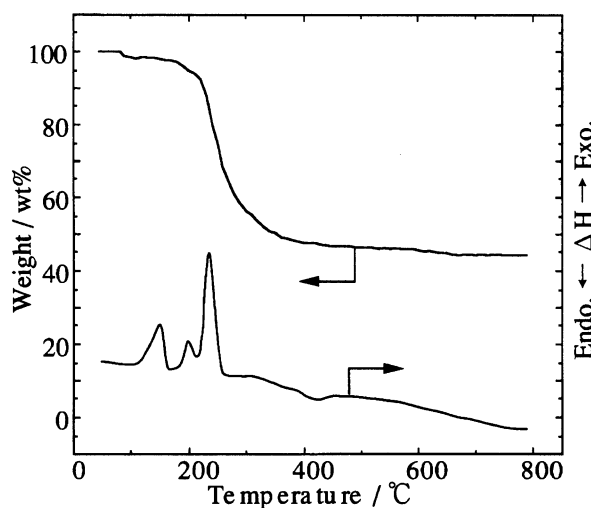
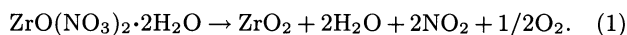


Fig. 10. DTA/TG curve of  $\text{ZrO}(\text{NO}_3)_2 \cdot 2\text{H}_2\text{O}$ . Heating rate: 10 °C  $\text{min}^{-1}$ ,  $\text{N}_2$  flow rate: 8  $\text{ml min}^{-1}$ .

complicated, i.e., three exothermic peaks were observed. Although these peaks appear to correspond to a loss of the water of absorption, crystallization, and partial decomposition of nitrate, the mechanism of the decomposition process at this low temperature region was not analyzed in detail. The significant weight decrease from 200 °C is attributed to the complete decomposition of nitrate oxide into oxide. The weight decrease ended at 600 °C with the formation of  $\text{ZrO}_2$ . The weight decrease from room temperature to 600 °C was almost equal to that expected from the following reaction:



The decomposition temperature of  $\text{ZrO}(\text{NO}_3)_2$  was higher than that of  $\text{Mn}(\text{NO}_3)_3$ , and almost agreed with

that for the desorption of NO from the Mn-Zr oxide. Thus, the absorption of the oxidized NO species in this mixed-oxide system mainly occurs at Zr sites via the formation of a nitrate oxide-like compound at or below 200 °C. However, the NO<sub>x</sub> species retained in the Mn-Zr oxide again desorbed in the gas phase from 300 °C. At 400 °C, most of the NO had already been released from the solid. The formation of stable nitrate oxide-like species is expected to be the reason for the large absorption capacity of the Mn-Zr oxide.

**Effect of the Preparation Method of Mn-Zr Oxide.** The Mn-Zr oxide powder was prepared by 4 different methods, and subjected to the NO absorption experiment (Fig. 11). The powder obtained by coprecipitation from nitrate solution, the standard preparation method in this study, gave the highest overall removal of NO. A sample prepared by the precursor method, in which citric acid was added to a metal nitrate solution, also exhibited a relatively large absorption capacity. The surface area after heating at 450 °C for 6 h was 117 m<sup>2</sup> g<sup>-1</sup> for the Mn-Zr oxide prepared by the sol-gel process using metal isopropoxides, which is smaller than the value obtained for the coprecipitated sample from the nitrate solution (185 m<sup>2</sup> g<sup>-1</sup>). The absorption curve for the sol-gel processed sample sharply decreased from the beginning of the reaction. The absorption capacity is, therefore, obviously larger for the sample coprecipitated from nitrate. The grain growth of oxide obtained from the sol-gel method appears to have occurred to reduce the surface area, leading to the separation of two metallic components.

Although the removal of NO was the gas-solid bulk

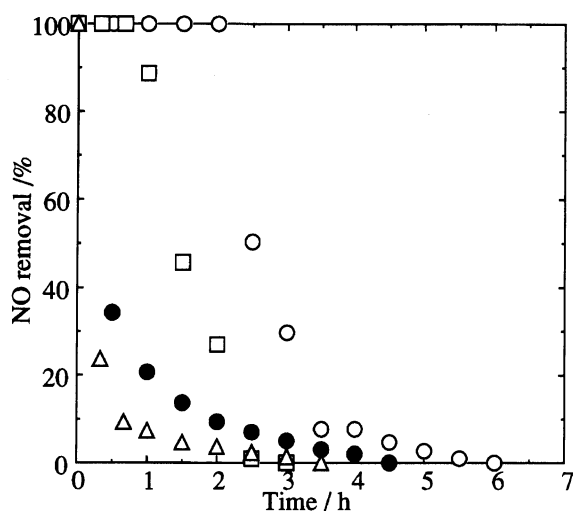


Fig. 11. NO removal of Mn-Zr oxides obtained by different preparation methods.  $T=200$  °C, 900 ppm NO, 10% O<sub>2</sub>, He balance,  $W/F=1$  g s cm<sup>-3</sup>. Samples were prepared by O coprecipitation from metal nitrates solution with ammonia. Δ coprecipitation from metal acetates solution with ammonia. □ coprecipitation from metal nitrates solution with an addition citric acid. ● hydrolysis of metal alkoxide.

reaction, as explained above, the absorption was initiated by a surface oxidation of the NO species. The surface area, therefore, significantly influences both the absorption rate and capacity. Only a limited part of the solid within a certain depth from the surface is expected to participate in the absorption reaction practically, since the absorption may accompany the diffusion of reacting species in the formed nitrate layer. The surface-to-volume ratio of the Mn-Zr oxide can be enhanced by depositing oxide fine particles on an oxide support with a large surface area. The absorption curve of NO for Mn-Zr oxide/Al<sub>2</sub>O<sub>3</sub> is shown in Fig. 12. The supported Mn-Zr oxide also exhibited a high removal of NO, which amounted to 4.91 cm<sup>3</sup> g<sup>-1</sup> or 1.214 mol/mol-Zr. Therefore, most of the Zr ions in the solid are expected to participate in the absorption of NO. A significant increase in the molar ratio of absorbed NO/Zr partially resulted from an enhancement in the surface area. However, small grains of Mn and Zr oxides formed by impregnation also brought about good mixing of both components at the surface so as to significantly enhance the absorption capacity.

### Conclusions

The present investigation indicated the possibility of Mn-Zr oxide as a new material for the absorption of NO<sub>x</sub>. The absorption-desorption behavior of solid has not been satisfactorily investigated because research involving NO<sub>x</sub> removal has been focused on the development of the catalytic process. However, the present system proposes the possibility of coupling the catalytic process with the separation process, which is based on the absorption-desorption cycle. The treatment of concentrated NO eliminates most of the difficulty encountered for the selective catalytic reduction of NO by hydrocarbons and catalytic NO decomposition. The ab-

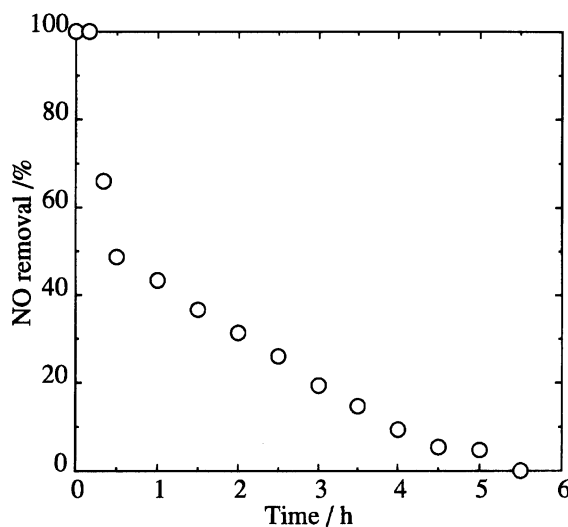


Fig. 12. Absorption curve of NO for 3.5 wt% Mn-Zr oxide supported on Al<sub>2</sub>O<sub>3</sub> at 200 °C. 900 ppm NO, 10% O<sub>2</sub>, He balance,  $W/F=1$  g s cm<sup>-3</sup>.

sorption of NO in the Mn-Zr oxide is very large in its amount, since the reaction is basically governed by the gas-solid reaction. However, the rate of removal is affected by the extent of mixing between the Mn- and Zr-oxides and the surface area of the mixed oxide. From this respect, the absorption material should be designed based on the control of the microstructure and component selection. The development of the system design is also necessary for the coupling of this absorption-desorption process and the catalytic-conversion steps.

## References

- 1) H. Hamada, Y. Kintaichi, M. Sasaki, and T. Ito, *Appl. Catal.*, **70**, L15-19 (1991).
  - 2) M. Misono and K. Kondo, *Chem. Lett.*, **1991**, 1001.
  - 3) M. Iwamoto, H. Yahiro, S. Shundo, Y. Yu-u, and N. Mizuno, *Appl. Catal.*, **69**, L15-L19 (1991).
  - 4) H. Hirabayashi, H. Yahiro, N. Mizuno, and M. Iwamoto, *Chem. Lett.*, **1992**, 2235.
  - 5) M. Yamato and M. Misono, *J. Chem. Soc., Chem. Commun.*, **1988**, 887.
  - 6) M. Machida, K. Yasuoka, K. Eguchi, and H. Arai, *J. Chem. Soc., Chem. Commun.*, **1990**, 1165.
  - 7) M. Saitou, T. Tachi, H. Yamashita, and H. Miyadera, *Nippon Kagaku Kaishi*, **1993**, 703.
  - 8) K. Eguchi, M. Watabe, S. Ogata, and H. Arai, *Shokubai (Catalyst)*, **36**, 108 (1994).
  - 9) C. C. Addison and B. M. Gatehouse, *J. Chem. Soc.*, **1960**, 613.
-